

Anisotropy of the Surface Impedance in the Surface-Sheath Regime as Evidence for Fluctuations of the Superconducting Order Parameter

KAZUMI MAKI

Department of Physics, Tôhoku University, Sendai, Japan

AND

GASTON FISCHER*

Département de Physique, Université de Montréal, Montréal 3, Canada

and

Laboratories RCA Ltd., CH 8005 Zurich, Switzerland

(Received 17 February 1969)

In the surface-sheath regime, the high-frequency surface impedance of a superconductor is a function of the angle between the polarization plane of the incident wave's electric vector \mathbf{E}_ω and the steady magnetic field \mathbf{H} . This anisotropy arises from collective fluctuations of the superconducting order parameter $\Delta(x)$. In the ground state $\Delta(x)$ is a nodeless function. When \mathbf{E}_ω and \mathbf{H} are perpendicular, the incident electromagnetic wave can couple to the intrinsic sheath currents and excite $\Delta(x)$ into states with a finite damping coefficient. No such excitations are possible when \mathbf{E}_ω and \mathbf{H} are parallel. The extra absorption predicted by theory in the dirty limit explains experimental data obtained from two lead-based alloys very well. These experiments should, therefore, be considered as direct evidence for the existence of collective fluctuations of the order parameter in the surface-sheath regime of superconductors.

I. INTRODUCTION

IN a previous paper,¹ to which we shall henceforth refer as I, we have reported surface resistance measurements on Pb-In and Pb-Bi alloys in the surface-sheath regime and presented a theoretical analysis of such measurements. In I, we have deliberately considered only the parallel situation, i.e., the configuration in which the static magnetic field \mathbf{H} is parallel to the plane of polarization of the electric microwave vector \mathbf{E}_ω , assumed to be incident perpendicularly on the plane sample surface (see Fig. 1).

The configuration in which \mathbf{H} and \mathbf{E}_ω are perpendicular to each other, but still both parallel to the sample surface, is of great interest for the following reasons: Caroli and Maki² have recently pointed out that in a superconductor of type II with the Abrikosov³ vortex structure there exists a class of collective fluctuations of the order parameter which appear, for example, as an anisotropy in the surface impedance. When the microwave electric vector \mathbf{E}_ω is parallel to the static magnetic field \mathbf{H} , the microwaves can not couple with these fluctuations. When, on the contrary, the polarization vector \mathbf{E}_ω is perpendicular to \mathbf{H} , the microwaves can excite a number of fluctuations and this results in an additional electromagnetic absorption. More recently one of us⁴ (K. M.) has performed a similar calculation

for the surface-sheath regime of dirty type-II superconductors. The reason why the microwaves can couple with the fluctuations of the surface sheath is easily apparent in Fig. 1, where it is seen that in the \perp geometry the intrinsic sheath currents $\mathbf{J}_s(x)$ flow in a direction parallel to the microwave electric vector \mathbf{E}_ω . In the \parallel geometry the vectors $\mathbf{J}_s(x)$ and \mathbf{E}_ω are \perp to each other, and they do not couple. In the vortex state, fluctuations of the order parameter are essentially the same thing as vibrations of the vortex lines in the superconductor. The condition for the microwaves to couple with these vibrations is that the induced microwave currents can exert a Lorentz force on the vortex lines.

In the numerical evaluation, use is made of the eigenvalues of the linearized Ginzburg-Landau equations, with the appropriate boundary conditions found by Fink and Kessinger.⁵ The calculation shows that there is an appreciable anisotropy of surface resistance $R(H)$ in the surface-sheath regime as well, according to the relative orientation of \mathbf{E}_ω and \mathbf{H} . In actual fact, the observation of the predicted anisotropy must be looked upon as a direct verification of the existence of these collective fluctuations.⁴

We believe that the surface-sheath regime has definite advantages over the vortex state of a type-II superconductor when testing the theory. In the vortex state it is not yet possible to take into account the modification of the Abrikosov³ vortex structure near the surface and this precludes, as shown already in I, any exact quantitative comparison. The anisotropy of $R(H)$ in the

* Present address: Département de Physique, Université de Montréal, Montréal 3, Can.

¹ G. Fischer and K. Maki, Phys. Rev. **176**, 581 (1968), referred to as I in text.

² C. Caroli and K. Maki, Phys. Rev. **159**, 306 (1967); **159**, 316 (1967).

³ A. A. Abrikosov, Zh. Eksperim. i Teor. Fiz. **32**, 1442 (1957) [English transl.: Soviet Phys.—JETP **5**, 1174 (1957)]. See also W. H. Kleiner, L. M. Roth, and S. H. Autler, Phys. Rev. **133**, A1226 (1964).

⁴ K. Maki, Progr. Theoret. Phys. (Kyoto) **39**, 1165 (1968). Note, however, that there is an error in this reference: The damping constant cited in Eq. (8), $\epsilon = 4.90\epsilon_0$ has to be corrected to

$\epsilon = 5.60\epsilon_0$. This correction applies to all subsequent calculations of the above reference. We should like to thank Dr. H. J. Fink for helpful correspondence on this point. Note that the effective damping constant is not the above ϵ , rather it is given by $\epsilon_1 = \epsilon - \epsilon_0$, as in Eq. (1) of the text.

⁵ H. J. Fink and R. D. Kessinger, Phys. Letters **25A**, 357 (1967), and H. J. Fink, Phys. Rev. **177**, 732 (1968).

surface-sheath regime was already noted⁶⁻⁹ long before the full theory of the fluctuations was available, but the attempts toward an explanation⁹ were not very satisfactory.

The aim of the present paper is both to present experimental data of the anisotropy, and to give a theoretical description of them in terms of the microscopic theory of superconductivity.^{10,11} We then compare experiment and theory.

In this paper we are not presenting a description of the experimental side of the work reported, since this has been done in detail in I to which we refer the reader.

II. THEORY OF THE SURFACE IMPEDANCE

In this section we set forth expressions for the surface impedance in the surface-sheath regime at magnetic fields H slightly below H_{c3} . Details of the derivation are given in the Appendix.

We consider here an experimental configuration as in Fig. 1 such that the metal occupies the half-space $x > 0$, the metal surface being then the plane $x=0$. A static magnetic field H slightly smaller than H_{c3} is applied in the z direction. In this situation, the equilibrium order parameter $\Delta_0(x)$ in a dirty type-II superconductor is given in terms of Saint-James and de Gennes's¹² solution. This solution is visualized as a nodeless solution, as in Fig. 1. However, the time-dependent Ginzburg-Landau equations predict the existence of a class of collective modes associated with fluctuations of the order parameter. The modes are simply damped in time like $\exp(-\epsilon_n t)$, where the modes with the longest lifetime have^{4,5}

$$\epsilon_1 = 4.60\epsilon_0, \quad \epsilon_2 = 10.5\epsilon_0, \quad \text{etc.}, \quad (1)$$

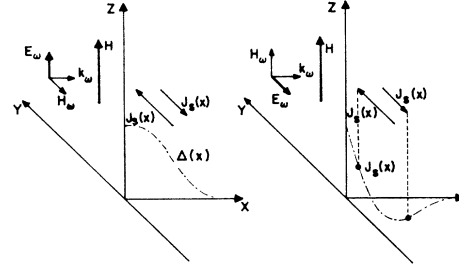
and where $\epsilon_0 = 1.18DeH_{c3}(t)$, with $D = \frac{1}{3}v_F l$ the electronic diffusion constant and $t = T/T_c$ the reduced temperature.

In considering the surface resistance, $R(H)$, it is very important to distinguish two different geometrical configurations:

(A) Parallel Geometry

This situation has been extensively discussed in I, where we found for the slope of $R(H)$ a discontinuity at $H = H_{c3}$ given by

$$s_3^{11}(t) = \left(\frac{H_{c3}}{R_n} \right) \frac{\partial R(H)}{\partial H} \Big|_{H=H_{c3}} = (2\pi)^{1/2} \left(\frac{\delta_0}{\xi(t)} \right) [2\kappa_2^2(t) - 0.334]^{-1}. \quad (2)$$



PARALLEL (\parallel) CONFIGURATION PERPENDICULAR (\perp) CONFIGURATION

FIG. 1. Sketch of the \parallel and \perp configurations. The microwaves are incident perpendicularly with the propagation vector \mathbf{k}_ω on the plane $x=0$. In the \parallel configuration the microwave electric vector E_ω is \parallel to the dc magnetic field \mathbf{H} and, thus, \perp to the intrinsic sheath currents $\mathbf{J}_s(x)$. In the perpendicular geometry, on the other hand, $\mathbf{E}_\omega \parallel \mathbf{J}_s(x)$. Note in the right-hand figure a sketch of $\mathbf{J}_s(x)$ and one of the order parameter $\Delta(x)$ in the left-hand figure.

In this formula $\delta_0 = (c^2/2\pi\omega\sigma)^{1/2}$ is the classical normal-state skin depth, σ the dc conductivity, $\omega/2\pi$ the frequency, and $\xi(t) = [\hbar c/1.18eH_{c3}(t)]^{1/2}$.

(B) Perpendicular Geometry

In this configuration we expect additional microwave absorption because of the excitation of collective fluctuations. This has the effect of reducing the slope of $R(H)$ at $H = H_{c3}$, or in other words, it reduces the discontinuity of the slope of $R(H)$ at H_{c3} . In the Appendix we find for this slope discontinuity

$$s_3^{\perp}(t) = \frac{H_{c3}}{R_n} \left(\frac{\partial R(H)}{\partial H} \right) \Big|_{H=H_{c3}} = A_3(t) (2\pi)^{1/2} \left(\frac{\delta_0}{\xi(t)} \right) [2\kappa_2^2(t) - 0.334]^{-1} \quad (3)$$

with

$$A_3(t) = 1 - \frac{2[\Psi(\frac{1}{2} + 5.60\rho) - \Psi(\frac{1}{2} + \rho)]}{(4.60)^2 \rho \Psi^{(1)}(\frac{1}{2} + \rho)}, \quad (4)$$

where $\Psi(z)$ and $\Psi^{(1)}(z)$ are the di- γ and tri- γ functions, and ρ is determined by

$$-\ln t = \Psi(\frac{1}{2} + \rho) - \Psi(\frac{1}{2}). \quad (5)$$

The right-hand term representing deviations from unity in Eq. (4) arises from the collective fluctuations. The temperature dependence of the anisotropy function $A_3(t)$ is given in Fig. 2 together with some experimental data. As the temperature decreases from T_c to zero, $A_3(t)$ increases from 0.565 to 0.84, i.e., the anisotropy is most prominent at higher temperatures.

In deriving Eqs. (3) and (4), we have made two major approximations⁴:

(a) We have assumed that only the first excited mode contributes to the absorption. A detailed numerical analysis shows that the neglect of the higher excited modes leads to an error of less than a few percent.

⁶ M. Cardona, G. Fischer, and B. Rosenblum, Phys. Rev. Letters **12**, 101 (1964).

⁷ M. Cardona and B. Rosenblum, Phys. Letters **8**, 308 (1964).

⁸ B. Rosenblum and M. Cardona, Phys. Letters **9**, 220 (1964).

⁹ G. Fischer and R. Klein, Phys. Rev. **165**, 578 (1968).

¹⁰ K. Maki, Physics (N. Y.) **1**, 21 (1964).

¹¹ P. G. de Gennes, Physik Kondensierten Materie **3**, 79 (1964).

¹² D. Saint-James and P. G. de Gennes, Phys. Letters, **7**, 306 (1963).

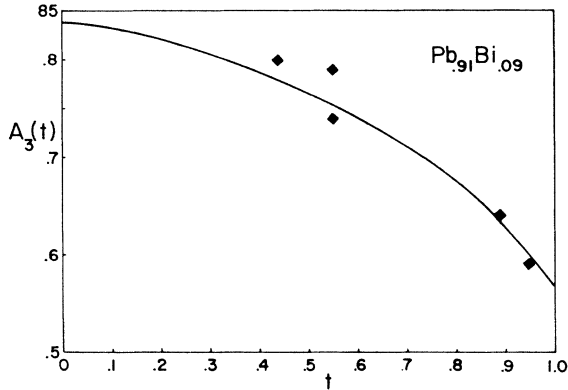


FIG. 2. Anisotropy function $A_3(t)$ defined by Eq. (4) of the text. The full diamonds are experimental data from a $\text{Pb}_{0.91}\text{Bi}_{0.09}$ alloy sample (sample No. 1).

(b) For the equilibrium order parameter there is equipartition of energy between kinetic and potential energy, just like in the ground-state wave function of a harmonic oscillator.

The second assumption is necessary in evaluating the matrix element associated with the coupling of the microwaves to the first excited mode.

Making use of the above expressions we can analyze the surface resistance data directly with Eq. (3), or indirectly by taking the ratio $s_3^\perp(t)/s_3^{\parallel}(t)$ and comparing it with the anisotropy function $A_3(t)$.

III. COMPARISON BETWEEN EXPERIMENT AND THEORY

From the experimental $R(H)$ curves we have deduced $s_3^{\parallel}(t)$ and $s_3^\perp(t)$ by taking the derivatives $\partial R(H)/\partial H$ at $H = H_{c3}$. The solid line for $s_3^{\parallel}(t)$ in Fig. 3 is taken from I and the solid line for $s_3^\perp(t)$ represents expression (3), i.e., the product of the experimental $s_3^{\parallel}(t)$ from sample No. 1 and the calculated $A_3(t)$. The experimental data points for $s_3^\perp(t)$ are from two samples: The full diamonds are uncorrected data from sample No. 1, and the open circles are data obtained from sample No. 2 after multiplication by a factor of 1.10. From the plot of Fig. 3 we see, then, that data obtained from one and the same sample for $s_3^{\parallel}(t)$ and $s_3^\perp(t)$ are in excellent agreement with the theoretical prediction without any sort of adjustment being made anywhere. This is particularly evident in Fig. 2, which reproduces both the theoretical result for the anisotropy function $A_3(t)$ as given by Eq. (4) and the uncorrected experimental ratios $s_3^\perp(t)/s_3^{\parallel}(t)$ for sample No. 1. Unfortunately sample No. 1 was destroyed while attempts were made to mount it into a cavity more suited to measurements of $s_3^\perp(t)$, and this explains the scarcity of data points from this sample.

The uncorrected results from sample No. 2, on the other hand, are about 10% below the predictions of the theory, i.e., we obtain a larger anisotropy than expected. We do not know the origin of this discrepancy, but

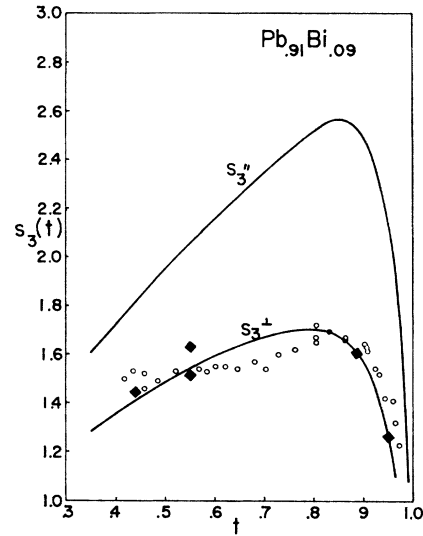


FIG. 3. The functions $s_3^{\parallel}(t)$ and $s_3^\perp(t)$. $s_3^{\parallel}(t)$ is the experimental curve for $\text{Pb}_{0.91}\text{Bi}_{0.09}$ sample No. 1 and is taken from I. $s_3^\perp(t)$ is the curve calculated from the above $s_3^{\parallel}(t)$ and $A_3(t)$ of Fig. 2 and Eq. (4). The full diamonds are uncorrected data from sample No. 1 and the open circles are 1.10 times the experimental $s_3^\perp(t)$ data from sample No. 2.

suspect sample No. 2 to be of poorer quality. We hope to be able to clarify this point in the future.

It is interesting to note that, whereas strong-coupling effects appear markedly in the large temperature dependence of $\kappa_2(t)$, and therefore also in $s_3^{\parallel}(t)$ and $s_3^\perp(t)$, they do not seem to influence the anisotropy ratio $A_3(t)$.

ACKNOWLEDGMENT

We are very grateful to Dr. H. J. Fink for providing us with some unpublished numerical data relating to the damping coefficient of the various collective modes of the surface sheath and the matrix elements for the transitions between modes.

APPENDIX: CALCULATION OF THE SURFACE IMPEDANCE IN THE PERPENDICULAR GEOMETRY

We assume that the superconductor occupies the half-space $x > 0$ and that the dc magnetic field \mathbf{H} is applied parallel to the surface, pointing in the z direction. The monochromatic plane polarized microwave is incident perpendicularly to the surface, with its electric vector \mathbf{E}_ω perpendicular to \mathbf{H} . In this situation the microscopic calculation leads to the following expression⁴ for the current induced by the microwave vector potential¹³

$$j_\omega(\mathbf{r}) = Q_1(\mathbf{r}, \omega) A_\omega(\mathbf{r}) \quad (\text{A1})$$

with

$$Q_1(\mathbf{r}, \omega) = Q_{11}(\mathbf{r}, \omega) + R(\mathbf{r}, \omega). \quad (\text{A2})$$

¹³ The calculation presented in the Appendix is carried out in a system of units such that $\hbar = k_B = c = 1$, and with a time dependence of the form $\exp(+i\omega t)$.

$Q_{11}(\mathbf{r}, \omega)$ is the same function as in I and $R(\mathbf{r}, \omega)$ is given by the expression, assuming variation only along coordinate x ,

$$R(x, \omega) = -2\sigma D(2eH_{c3})^2(x-x_0)^2 |\Delta(x)|^2 \left[\Psi\left(\frac{1}{2} - \frac{i\omega}{4\pi T} + 5.60\rho\right) - \Psi\left(\frac{1}{2} + \rho\right) \right]^{-1} \\ \times \left\{ \frac{1}{4.60\epsilon_0 - i\omega} \left[\Psi\left(\frac{1}{2} - \frac{i\omega}{4\pi T} + 5.60\rho\right) - \Psi\left(\frac{1}{2} + \rho\right) \right] \right. \\ \left. + \frac{1}{4.60\epsilon_0 + i\omega} \left[\Psi\left(\frac{1}{2} - \frac{i\omega}{4\pi T} + 5.60\rho\right) - \Psi\left(\frac{1}{2} - \frac{i\omega}{2\pi T} + \rho\right) \right] \right\}^2, \quad (A3)$$

where σ is the normal-state dc conductivity,

$$\rho = \epsilon_0/4\pi T, \quad \epsilon_0 = 1.18DeH_{c3}(t), \quad D = \frac{1}{3}v_F l$$

is the electronic diffusion constant, and $\Psi(z)$ and $\Psi^{(1)}(z)$ are the di- and tri- γ functions. $\Delta(\mathbf{r})$ is the space-dependent order parameter, $x_0 = k/2eH_{c3}$ and k is associated with the y dependence of $\Delta(\mathbf{r})$ as given by

$$\Delta(\mathbf{r}) = e^{iky} f(x).$$

Expression (A2) is valid in the surface-sheath regime near H_{c3} (i.e., $H_{c3} - H \ll H_{c3}$) and with $\Delta(\mathbf{r})$ as first calculated by Saint-James and de Gennes.¹²

It is interesting to note that the term associated with $R(\mathbf{r}, \omega)$ comes from collective fluctuations of the order parameter in the surface-sheath regime and this term is present only in the perpendicular geometry. More precisely speaking, if the polarization vector \mathbf{E}_ω has an angle θ to the dc magnetic field, we can still describe the response by (A1) but now $Q_{11}(\mathbf{r}, \omega)$ has a similar form as (A2) with the term $R(\mathbf{r}, \omega)$ multiplied by a factor $\sin^2\theta$. In particular, in the parallel geometry (i.e., $\mathbf{E}_\omega \parallel \mathbf{H}$, which is the situation treated in I), we have no contribution from the collective fluctuations of the order parameter.

In order to calculate the surface impedance, we have to solve the differential equation

$$-\frac{\partial^2 A_\omega(x)}{\partial x^2} = 4\pi Q(x, \omega) A_\omega(x), \quad (A4)$$

with appropriate boundary conditions. The surface impedance is then given by

$$Z = R + iX = 4\pi \frac{E_\omega(0)}{H_\omega(0)} = -4\pi i\omega \frac{A_\omega(x)}{\partial A_\omega(x)/\partial \omega} \Big|_{x=0}. \quad (A5)$$

The solution of (A4) in the surface-sheath regime has been discussed in detail in I. Making use of the same method, we can express the surface impedance as

$$Z = 4\pi i\omega / [b + \varphi'(0)], \quad (A6)$$

where

$$b^{-1} = \delta_0 / (1+i), \quad \delta_0 = (2\pi\omega\sigma)^{-1/2}, \quad (A7)$$

$$\varphi'(x) = 4\pi\sigma e^{2bx} \int_x^\infty e^{-2bx'} f_1(x') dx',$$

and

$$f_1(x', \omega) = f_{11}(x', \omega) - R(x', \omega) / \sigma. \quad (A8)$$

For $f_{11}(x', \omega)$ we have

$$f_{11}(x', \omega) = \frac{|\Delta(x')|^2}{2\pi T} \left\{ \Psi^{(1)}\left(\frac{1}{2} - \frac{i\omega}{2\pi T} + \rho\right) + \left(\frac{2\pi T}{-i\omega} + \frac{2\pi T}{-i\omega + \epsilon_0}\right) \times \left[\Psi\left(\frac{1}{2} - \frac{i\omega}{2\pi T} + \rho\right) - \Psi\left(\frac{1}{2} + \rho\right) \right] \right\}.$$

In the microwave experiment the frequency ω is much smaller than $\epsilon_0(0) = 1.18DeH_{c3}(0)$. We can, therefore, expand (A8) in powers of ω and retain only the term independent of ω ; $f_1(x)$ can then be approximated by

$$f_1(x) \cong \frac{|\Delta(x)|^2}{\pi T} \Psi^{(1)}\left(\frac{1}{2} + \rho\right) - \frac{8D(2eH_{c3})^2}{(4.60\epsilon_0)^2} (x-x_0)^2 |\Delta(x)|^2 \times [\Psi\left(\frac{1}{2} + 5.60\rho\right) - \Psi\left(\frac{1}{2} + \rho\right)] + O\left(\frac{\omega}{\epsilon_0(0)}\right). \quad (A9)$$

Substituting (A9) in (A7) we find

$$\varphi'(0) \cong 4\pi\sigma \int_0^\infty f(x') dx' = [(2\pi)^{1/2} / \xi(t)] (1 - H/H_{c3}) \times [2\kappa_2^2(t) - 0.334]^{-1} A_3(t), \quad (A10)$$

where

$$A_3(t) = 1 - \frac{2[\Psi\left(\frac{1}{2} + 5.60\rho\right) - \Psi\left(\frac{1}{2} + \rho\right)]}{(4.60)^2 \rho \Psi^{(1)}\left(\frac{1}{2} + \rho\right)}. \quad (A11)$$

In the estimation of the above integral we have approximated $\Delta(x)$ with the Gaussian form

$$|\Delta(x)| = |\Delta(0)| \exp(-x^2/2\xi^2(t)), \quad (A12)$$

and also made use of the normalization of $\langle |x|^2 \rangle_{av}$ determined from the generalized Ginzburg-Landau equations,¹⁰

$$\langle |\Delta|^2 \rangle_{av} = \left(\frac{1}{2}\pi\right)^{1/2} \frac{0.59eT}{\sigma} \times \frac{H_{c3} - H}{2\kappa_2^2(t) - 0.334} [\Psi^{(1)}(\frac{1}{2} + \rho)]^{-1}. \quad (A13)$$

Finally, the surface impedance is given by

$$Z \cong R_n \left\{ 1 + i - (2\pi)^{1/2} \left(\frac{\delta_0}{\xi(t)} \right) A_3(t) \left(\frac{H_{c3} - H}{H_{c3}} \right) \times [2\kappa_2^2(t) - 0.334]^{-1} \right\}, \quad (A14)$$

and from (A14) we can derive $s_3^{\pm}(t)$:

$$s_3^{\pm}(t) = \frac{H_{c3}}{R_n} \left(\frac{\partial R(H)}{\partial H} \right) \Big|_{H=H_{c3}} = (2\pi)^{1/2} \left(\frac{\delta_0}{\xi(t)} \right) \frac{A_3(t)}{2\kappa_2^2(t) - 0.334}. \quad (A15)$$

It is also very easy to repeat the calculation for the configuration when the polarization vector \mathbf{E}_ω of the microwaves spans an angle θ with the dc magnetic field \mathbf{H} . A calculation similar to the one just performed gives

$$s_3(t, \theta) = (2\pi)^{1/2} \left(\frac{\delta_0}{\xi(t)} \right) \frac{A_3(t, \theta)}{2\kappa_2^2(t) - 0.334}, \quad (A16)$$

and

$$A_3(t, \theta) = 1 - \sin^2 \theta \frac{2[\Psi(\frac{1}{2} + 5.60\rho) - \Psi(\frac{1}{2} + \rho)]}{(4.60)^2 \rho \Psi^{(1)}(\frac{1}{2} + \rho)}. \quad (A17)$$

Gamma-Irradiation Effects in Single-Crystalline Barium Titanate

JOHN J. KEATING* AND GLENN MURPHY

Department of Nuclear Engineering, Iowa State University of Science and Technology, Ames, Iowa 50010

(Received 6 August 1968; revised manuscript received 24 February 1969)

This study presents the results of an experimental investigation of Co^{60} γ -irradiation effects in single-crystalline barium titanate. Two test groups of crystals were utilized in this study. Prior to being irradiated, one group was etched in phosphoric acid at 145°C to remove a surface layer having properties which differ from the bulk of the crystal. The second group of crystals was irradiated in the as-grown condition. Following irradiation at various γ doses, the ferroelectric hysteresis loop was determined, measurements were taken of the optical absorption spectrum in the wavelength range 0.43–0.70 μ , and photomicrographs of the domain structure were obtained. The temperature was maintained at 20°C during irradiation, and all post-irradiation measurements were made at 23°C. The etched crystals were irradiated in the poled condition to a maximum dose of 1.60×10^9 rad. The remanent polarization P_r was unaffected by a total γ dose of about 2×10^8 rad. Irradiation to higher dose levels caused a reduction in P_r . The coercive field E_c was reduced with initial irradiation. At a dose of about 5×10^8 rad, a minimum value was reached and E_c then increased with continued irradiation. The domain structure of the c -domain crystals was unaffected by a total γ dose of 1.60×10^9 rad. No absorption peaks were observed in the wavelength range studied as a result of Co^{60} γ irradiation. The radiation-induced changes observed in the ferroelectric hysteresis loop of etched crystals cannot be attributed to changes in the domain structure or to the presence of point defects consisting of an oxygen vacancy with a single trapped electron. The unetched crystals were irradiated to a maximum dose of 2.91×10^8 rad. With initial irradiation, the polarization reversal process was enhanced as the remanent polarization increased and the coercive field decreased. With increasing dose above 2×10^7 rad, the hysteresis loop gradually deteriorated. The unetched crystals were found to be much more sensitive to Co^{60} γ radiation than were the etched crystals.

I. INTRODUCTION

THE details of radiation effects upon the electrical properties of single-crystalline barium titanate are not well understood. A few investigations have been reported; however, in most cases the results are not consistent or in good agreement. The disagreement of

experimental results has limited the development of a satisfactory model for radiation damage in BaTiO_3 .

Lefkowitz and Mitsui¹ studied the effect of Co^{60} γ -ray and reactor irradiation on the hysteresis loop of single-crystalline BaTiO_3 . For a neutron ($E > 0.4$ eV) dosage of $2.8 \times 10^{16} n/\text{cm}^2$, they observed a decrease in coercive field and an increase in spontaneous polarization. Similar

* Present address: U. S. Atomic Energy Commission Idaho Operations Office, Idaho Falls, Idaho.

¹ I. Lefkowitz and T. Mitsui, J. Appl. Phys. **30**, 269 (1959).